

Evidence for selenocysteine coordination to the active site nickel in the [NiFeSe]hydrogenases from *Desulfovibrio baculatus*

(x-ray absorption spectroscopy/TGA codon/ $^2\text{H}_2\text{-H}^+$ exchange)

MARLY K. EIDSNES*, ROBERT A. SCOTT*†, BENET C. PRICKRIL*, DANIEL V. DERVARTANIAN*, JEAN LEGALL*, ISABEL MOURA‡, JOSE J. G. MOURA‡, AND HARRY D. PECK, JR.*

*Departments of Chemistry and Biochemistry and the Center for Metalloenzyme Studies, University of Georgia, Athens, GA 30602; and ‡Centro de Quimica Estrutural, Universidade Nova de Lisboa, Avenue Rovisco Pais, 1000 Lisbon, Portugal

Communicated by Harry B. Gray, September 1, 1988 (received for review June 9, 1988)

ABSTRACT Ni and Se x-ray absorption spectroscopic studies of the [NiFeSe]hydrogenases from *Desulfovibrio baculatus* are described. The Ni site geometry is pseudo-octahedral with a coordinating ligand composition of 3–4 (N,O) at 2.06 Å, 1–2 (S,Cl) at 2.17 Å, and 1 Se at 2.44 Å. The Se coordination environment consists of 1 C at 2.0 Å and a heavy scatterer M (M = Ni or Fe) at ≈ 2.4 Å. These results are interpreted in terms of a selenocysteine residue coordinated to the Ni site. The possible role of the Ni–Se site in the catalytic activation of H_2 is discussed.

Hydrogenases are vital to the anaerobic metabolism of sulfate-reducing bacteria and many other types of bacteria. Hydrogenases catalyze the bidirectional activation of molecular hydrogen



and their activities are routinely determined by H_2 production, H_2 utilization, or the $^2\text{H}_2\text{-H}^+$ exchange assays (1). In the past, it was generally accepted that a single hydrogenase carried out these simple redox reactions (1), but in recent years the unveiling of the structural diversity of hydrogenases has promoted the idea that different hydrogenases may reflect differences in cellular localization and metabolic function (2). This specificity suggests that structural differences are the basis for tailoring the hydrogenase reaction to meet metabolic demands. The elucidation of the structural details of the active sites of hydrogenases is the first step toward a molecular understanding of the mechanisms involved in the hydrogenase reaction.

In the genus *Desulfovibrio*, the metabolism of hydrogen involves at least three types of hydrogenases that may be distinguished by their heavy element composition, immunological reactivities, and gene structures (3–6). The [Fe]hydrogenases contain only iron–sulfur clusters (7–9), the [NiFe]hydrogenases contain nickel and iron–sulfur clusters (10–15), and the [NiFeSe]hydrogenases contain iron–sulfur clusters and equimolar amounts of nickel and selenium (16, 17). The three types of hydrogenase as well as multiple forms of a single type of hydrogenase can occur within a single bacterium (18). In *Desulfovibrio baculatus*, three [NiFeSe]hydrogenases have been identified, based on their cellular locations: periplasmic, cytoplasmic, and membrane-bound. Electron paramagnetic resonance (EPR) studies indicate that these hydrogenases are spectroscopically distinct as isolated but under reducing conditions exhibit identical EPR signals (19).

A considerable amount of circumstantial evidence indicates that nickel is involved in the activation of H_2 by the Ni-containing hydrogenases; however, the [NiFe]- and [Ni-

FeSe]hydrogenases differ in some of their catalytic activities (19, 20) and sensitivities to inhibitors. These observations suggested the possibility that one of the sulfur ligands to the active site nickel is replaced by a selenium ligand in the [NiFeSe]hydrogenase.

As part of our effort to elucidate the structures of the nickel sites in the Ni-containing hydrogenases, and to define a structural basis for the functional differences between the Se- and the non-Se-containing hydrogenases (19, 20), we report here the results of Ni and Se x-ray absorption spectroscopic measurements on the [NiFeSe]hydrogenases of *D. baculatus*.

MATERIALS AND METHODS

Sample Preparation. The *D. baculatus* [NiFeSe]hydrogenase sample was prepared according to the procedure described in ref. 19. To obtain a sample ≈ 2 mM Ni and Se, the periplasmic, cytoplasmic, and membrane-bound fractions were combined. Total iron was determined by the 2,4,6-tripyridyl-1,3,5-triazine method (21), and metals were quantified by plasma emission spectroscopy using a Mark II Jarrell-Ash model 965 AtomComp (Fisher). Nickel was also determined by atomic absorption spectroscopy. The sample for x-ray absorption spectroscopy (XAS) was placed in a Lucite/Mylar cell, ≈ 80 μl in volume, and stored in liquid nitrogen until the time of data collection. The *Desulfovibrio gigas* [NiFe]hydrogenase sample preparation has been described (22). The structurally characterized Ni model compounds used for Ni K x-ray absorption edge region comparisons were [(C₆H₅)₄P]₂[Ni(SC₆H₅)₄] [a gift from D. Coucouvanis (23)], [Ni(TC-6,6)] [TC-6,6 = tropocoronand-(CH₂)₆, (CH₂)₆] [a gift from S. J. Lippard (24)], (R,S,R,S)-[Ni(tetramethylcyclam)Br](ClO₄) [a gift from J. H. Espenson and M. S. Ram (25, 26)], [Ni([9]aneN₃)₂](ClO₄)₂ ([9]aneN₃ = 1,4,7-triazacyclononane) (27, 28), and [Ni([9]aneS₃)₂](ClO₄)₂ ([9]aneS₃ = 1,4,7-trithiacyclononane) [a gift from K. Wieghardt (29)]. The Se model compounds used for comparison of Se K x-ray absorption edge regions were Fe₂Se₂(CO)₆ (30, 31), and selenocysteine and selenomethionine, both purchased from Sigma.

Data Collection. All XAS data were collected at the Stanford Synchrotron Radiation Laboratory on beam lines II-3, IV-1, or VII-3, using Si[220] monochromator crystals. Protein data were measured under dedicated operating conditions at 3.0 GeV, as were most model compounds, with the exception of some Se compounds measured at 2.0 GeV under parasitic conditions. At 3.0 GeV, typical electron currents were between 40 and 70 mA, and at 2.0 GeV, the current was ≈ 15 mA. Data were collected at ≈ 10 K with a continuous-flow liquid-helium cryostat (Oxford Instruments Model CF1208), except for some Se compounds measured at am-

bient temperature. Protein XAS spectra were collected in fluorescence mode with a Stern-Heald-Lytle type fluorescence detector (32) purchased from the EXAFS Co., Seattle. Model compound spectra were collected in transmission mode using N₂-filled ionization chambers. The model compound samples were prepared by diluting the finely ground powders approximately 1:3 with boron nitride to minimize the thickness effect (33). In general, 3 scans were collected on model compound samples, 3–5 scans for protein edge region spectra, and 15–28 scans for protein extended x-ray absorption fine structure (EXAFS) spectra.

Data Reduction and Analysis. Data reduction and analysis were performed according to our published procedures (34). For the curve-fitting analyses, the following theoretical expression for the EXAFS was used:

$$\chi(k) = \sum_s \frac{B_s N_s |f_s(\pi, k)|}{k R_{as}^2} \exp(-2\sigma_{as}^2 k^2) \sin[2kR_{as} + \alpha_{as}(k)]. \quad [1]$$

For each shell of scatters, s , N_s is the number of scatters at an average distance R_{as} from the absorbing atom (Ni or Se). σ_{as} is the root-mean-square deviation in R_{as} , which takes into account both static and thermal disorder. The simulated EXAFS (from Eq. 1) was adjusted to fit the observed EXAFS

by allowing the R_{as} and σ_{as} values for each shell to vary in a nonlinear least-squares optimization. In each shell, the type of scattering atom was chosen by selection of the appropriate backscattering function, appearing in Eq. 1 as amplitude $[B_s |f_s(\pi, k)|]$ and phase $[\alpha_{as}(k)]$ components. When $|f_s(\pi, k)|$ was taken from theoretical tables (35), B_s was adjusted to give satisfactory fits to the EXAFS of structurally characterized model compounds.

The backscattering functions for the absorber–scatterer pairs, Ni–N, Ni–S, and Ni–Se were extracted from [Ni–{(imid)₂biphen}₂](ClO₄)₂ [(imid)₂biphen] = 2,2′-bis(2-imidazolyl)biphenyl] [a gift from H. J. Schugar (36)], [(C₄H₉)₄N][Ni(mnt)₂] (mnt=maleonitriledithiolate) (37, 38), and [(C₄H₉)₄N][Ni{Se₂C₂(CF₃)₂}]₂ [a gift from B. M. Hoffman (39)], respectively. E_0 for the onset of the Ni EXAFS was chosen to be 8350 eV. Se scattering functions were taken from theoretical tables (35), with subsequent refinement of B_s and ΔE_0 for each absorber–scatterer pair. Se–C, Se–Fe, and Se–Ni scattering functions were from PhSeSePh (Ph=phenyl) (40), Fe₂Se₂(CO)₆ (30, 31), and [(C₄H₉)₄N][Ni{Se₂C₂(CF₃)₂}]₂ (39), respectively, yielding B_s , ΔE_0 values of 0.5, –23.6 eV; 0.6, +9.0 eV; and 0.5, –3.3 eV, respectively. E_0 for the Se EXAFS was chosen to be 12,675.0 eV.

RESULTS

Ni Edges. The edge region of the Ni *K* edge x-ray absorption spectrum generally reveals considerable information about the electronic and molecular structure of the Ni site (41). In Fig. 1 we compare the edge spectra of the *D. baculatus* [NiFeSe] and the *D. gigas* [NiFe]hydrogenases and several structurally characterized Ni model compounds. The signature for tetrahedral geometry is the presence of a weak but well-resolved $1s \rightarrow 3d$ pre-edge transition at ≈ 8332 eV (Fig. 1, spectrum a) (41). In the case of approximate square-planar symmetry, an intense pre-edge transition is observed at ≈ 8336 eV (spectrum e), ascribed to the $1s \rightarrow 4p_z$ (or $1s \rightarrow 4p_z$ plus shakedown) transition (42). In contrast to these readily observable transitions, octahedral geometry is characterized by a rather featureless pre-edge region (spectrum d). The edge spectrum of a pentacoordinate NiN₄Br compound (spectrum b) has features of both tetrahedral and octahedral edges: a weak but well-resolved $1s \rightarrow 3d$ transition at ≈ 8332 eV (similar to but less intense than in the edge of the

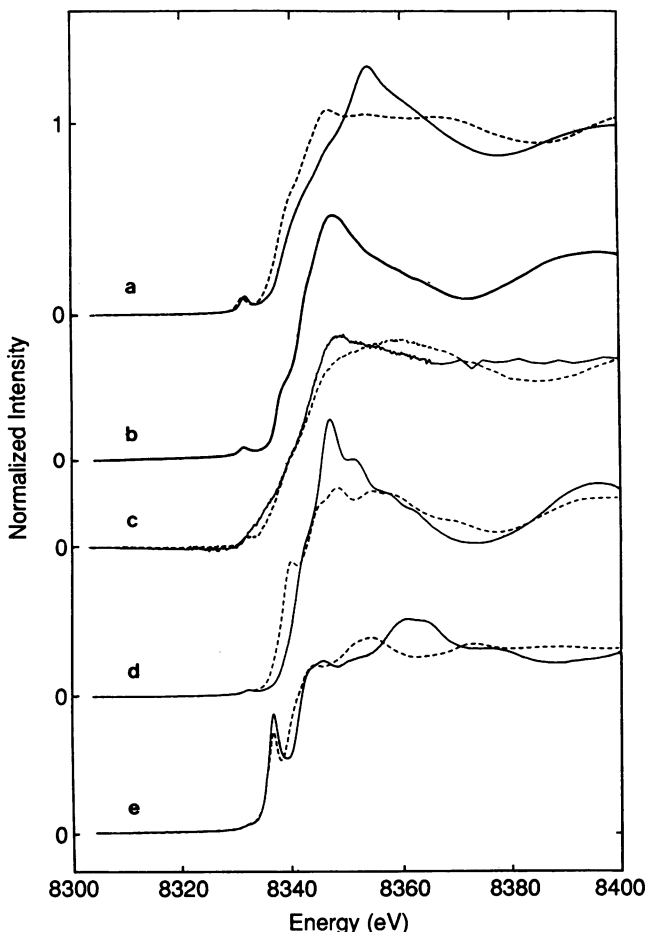


FIG. 1. Ni *K* edge region spectra of *D. gigas* [NiFe]- and *D. baculatus* [NiFeSe]hydrogenases, compared to various model compounds. Spectra: a, approximately tetrahedral NiN₄ compound, Ni[tropocoronand-(CH₂)₆, (CH₂)₆] (—), and tetrahedral NiS₄ compound, [Ni(SC₆H₅)₄]²⁻ (---); b, pentacoordinate NiN₄Br compound, [Ni(tetramethylcyclam)Br]⁺; c, oxidized (as isolated) hydrogenases from *D. baculatus* (—) and *D. gigas* (---); d, approximately octahedral NiN₆ and NiS₆ compounds, [Ni(1,4,7-triazacyclononane)]₂²⁺ (—) and [Ni(1,4,7-trithiacyclononane)]₂²⁺ (---); e, approximately square-planar NiS₄ and NiSe₄ compounds, [Ni(S₂C₄N₂)₂]²⁻ (—) and [Ni{Se₂C₂(CF₃)₂}]⁻ (---).

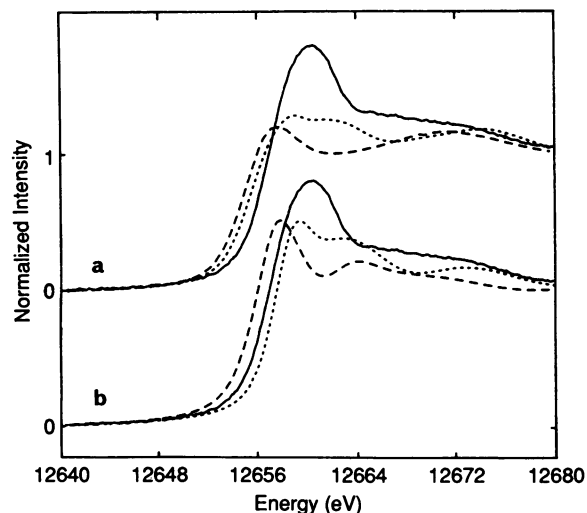


FIG. 2. Se *K* edge spectra of *D. baculatus* [NiFeSe]hydrogenase compared to various Se compounds. Spectra: a, oxidized (as isolated) *D. baculatus* hydrogenase (—), Fe₂Se₂(CO)₆ (---), [Ni{Se₂C₂(CF₃)₂}]⁻ (---); b, oxidized (as isolated) *D. baculatus* hydrogenase (—), selenocystine (---), and selenomethionine (---).

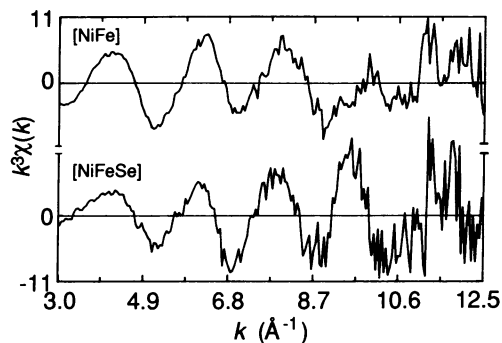


FIG. 3. Raw Ni EXAFS of *D. gigas* [NiFe]- (Upper) and *D. baculatus* [NiFeSe]- (Lower) hydrogenases. The general increase in EXAFS amplitude near $k = 9 \text{ \AA}^{-1}$ suggests the presence of heavier scatterers in the [NiFeSe]hydrogenase data.

tetrahedral compound), a shoulder at $\approx 8338 \text{ eV}$ that may be a poorly resolved $1s \rightarrow 4p_z$ transition, and a pronounced broad peak at the edge maximum (similar to but less intense than that of the NiN_6 pseudo-octahedral edge). By comparison, the [NiFeSe]- and [NiFe]hydrogenase edges shown in spectrum c suggest that the Ni sites are either pseudo-octahedral or possibly pentacoordinate. Distinct differences in the hydrogenase Ni edges exist, however, and they indicate a difference in ligands or symmetry or both between the [NiFeSe]- and [NiFe]hydrogenase Ni sites.

Se Edges. In contrast to the various pre-edge transitions of the Ni edge region, the edge region of the Se K edge x-ray absorption spectrum exhibits no pre-edge transitions (Se having a closed $3d$ shell electronic configuration). Fig. 2 shows the Se edge spectra of the [NiFeSe]hydrogenases and various Se compounds. Despite the lack of information available from any pre-edge transitions, one may make use of the sensitivity of the edge inflection point to the charge density of the absorbing atom. For example, a change in oxidation state or a change in the degree of covalent character in the metal-ligand bond may shift the edge energy.

The energy of the edge inflection point varies among the model compounds by $\approx 3 \text{ eV}$, the highest energy inflection point occurring in the selenomethionine spectrum (Fig. 2, spectrum b, dotted line). In selenomethionine, the Se atom is bound covalently to C atoms exclusively. In the other model compounds, Se is bound to higher Z elements and the corresponding edge spectra have inflection points at lower energies: selenocystine (spectrum b, dashed line) contains a Se-Se bond, $[\text{Ni}\{\text{Se}_2\text{C}_2(\text{CF}_3)_2\}_2]^-$ (spectrum a, dotted line)

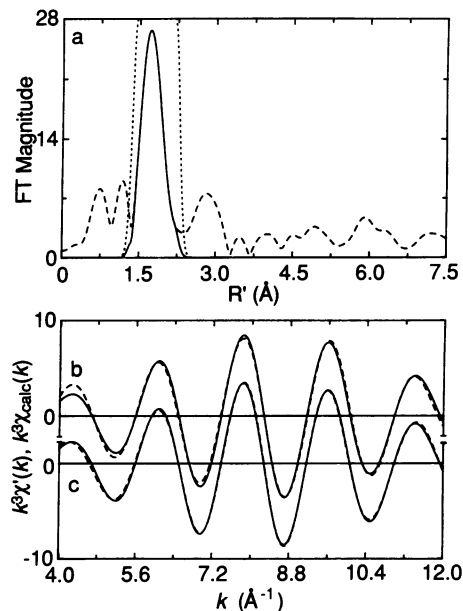


FIG. 4. (a) Fourier transform (FT) of Ni EXAFS of oxidized (as isolated) *D. baculatus* [NiFeSe]hydrogenase ($k = 3.0 - 12.5 \text{ \AA}^{-1}$, k^3 weighting), showing the filter (dotted line) of the first-shell FT peak. The solid lines in b and c are the first-shell filtered EXAFS data and the dashed lines are two curve-fitting simulations, using the structural parameters from fits 1D (b) and 1F (c) (see Table 1).

contains a Se-Ni bond, and $\text{Fe}_2\text{Se}_2(\text{CO})_6$ (spectrum a, dashed line) has both Se-Fe and Se-Se bonds. The Se edge of the [NiFeSe]hydrogenase falls at an intermediate energy, 2.3 eV below the selenomethionine edge. This suggests that Se is not coordinated exclusively to low Z elements.

Ni EXAFS. Fig. 3 compares the raw Ni EXAFS data of the [NiFeSe]- and [NiFe]hydrogenases. The increase in the EXAFS amplitude in the [NiFeSe]hydrogenase data near $k = 9 \text{ \AA}^{-1}$ suggests the presence of a heavy scatterer not observed in the [NiFe]hydrogenase EXAFS. The Ni EXAFS data for [NiFeSe]hydrogenase were Fourier filtered as shown in Fig. 4a, and curve-fitting results are shown in Fig. 4b and c and Table 1. Examination of the goodness-of-fit (f') values in Table 1 shows that including only Ni-(N,O) and Ni-(S,Cl) shells in the simulation (fits 1A-1D) does not adequately fit the observed data, even if two separate shells of Ni-(S,Cl) are used in three-shell fits (fits 1C, 1D; Fig. 4b). Three-shell fits including Ni-(N,O), Ni-(S,Cl), and Ni-Se shells improve the

Table 1. Curve-fitting results for Ni EXAFS of *D. baculatus* hydrogenase

Fit	Ni-(N,O)			Ni-(S,Cl)			Ni-Se			f'
	N_s	R_{as} (Å)	$\Delta\sigma_{as}^2$ (Å ²)	N_s	R_{as} (Å)	$\Delta\sigma_{as}^2$ (Å ²)	N_s	R_{as} (Å)	$\Delta\sigma_{as}^2$ (Å ²)	
1A	(3)	2.07	-0.0043	(3)	2.19	0.0042	—	—	—	0.039
1B	(4)	2.07	-0.0022	(2)	2.19	0.0008	—	—	—	0.041
1C	(2)	2.03	-0.0060	(2)	2.24	0.0012	—	—	—	0.019
ID	(3)	2.03	-0.0043	(2)	2.23	-0.0007	—	—	—	0.022
				(1)	1.99	0.0025	—	—	—	
1E	(3)	2.06	-0.0047	(2)	2.19	0.0098	(1)	2.44	0.0049	0.011
1F	(4)	2.07	-0.0038	(1)	2.15	0.0003	(1)	2.45	0.0044	0.011
1G	(5)	2.05	-0.0027	—	—	—	(1)	2.43	0.0034	0.039

N_s is the number of scatterers per nickel; R_{as} is the nickel-scatterer distance; σ_{as} is a root-mean-square deviation in R_{as} ; $\Delta\sigma_{as}^2$ is $\sigma_{fit}^2 - \sigma_{model}^2$, where the models for Ni-N, Ni-S, and Ni-Se were $\{\text{Ni} [2,2'-\text{bis}(2\text{-imidazolyl})\text{biphenyl}]_2\}^{2+}$ at 4 K, $[\text{Ni}(\text{maleonitriledithiolate})_2]^-$ at 4 K, and $[\text{Ni}\{\text{Se}_2\text{C}_2(\text{CF}_3)_2\}_2]^-$ at 10 K, respectively. The k range of the fits was 4-12 \AA^{-1} . f' is a goodness-of-fit statistic normalized to the overall magnitude of the $k^3\chi(k)$ data:

$$f' = \frac{[\sum (k^3(\chi_{\text{obsd}}(k) - \chi_{\text{calc}}(k)))^2 / N]^{1/2}}{(k^3\chi)_{\text{max}} - (k^3\chi)_{\text{min}}}$$

Numbers in parentheses were not varied during optimization.

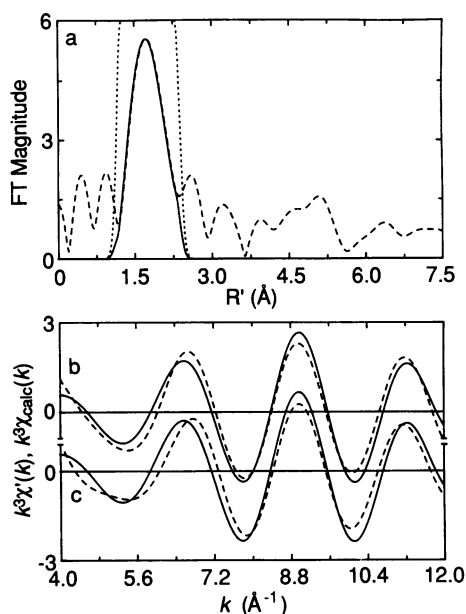


FIG. 5. (a) FT of Se EXAFS of oxidized (as isolated) *D. baculatus* [NiFeSe]hydrogenase ($k = 3.0 - 11.0 \text{ \AA}^{-1}$, k^3 weighting), showing the filter (dotted line) of the first-shell FT peak. The solid lines in *b* and *c* are the first-shell filtered EXAFS data and the dashed lines are two curve-fitting simulations, using the structural parameters from fits 2A (*b*) and 2B (*c*) (see Table 2).

fits (1E, 1F; Fig. 4c), yielding a single Se scatterer at a Ni–Se distance of 2.44 Å.

Se EXAFS. Corroborative evidence for the proposed Ni–Se bond should be available from the Se EXAFS. The position, size, and width of the Se EXAFS FT peak in Fig. 5a suggest the presence of a heavy scatterer, and curve-fitting clearly demonstrates that one or two Se–C interactions alone cannot reproduce this EXAFS. Table 2 lists two plausible Se EXAFS simulations and the fits are displayed in Fig. 5 *b* and *c*. Although the fits are not as good as the Ni EXAFS fits, due to the decreased signal/noise ratio of the Se EXAFS data and shorter Se EXAFS data range ($k = 4-10 \text{ \AA}^{-1}$), a heavy scatterer ($M = \text{Ni or Fe}$) is identified at a Se–M distance of 2.39 or 2.34 Å, respectively. Reasonable fits also require the presence of a Se–C interaction (Table 2).

DISCUSSION

The Ni and Se *K* edge x-ray absorption spectroscopic data have allowed us to define an approximate coordination structure for the Ni site in the *D. baculatus* [NiFeSe]hydrogenase. As for the *D. gigas* [NiFe]hydrogenase, the Ni site geometry is pseudo-octahedral with a mixture of (N,O)- and (S,Cl)-containing ligands (22). The Ni edge and EXAFS analyses in combination suggest that the [NiFeSe]hydrogenase Ni site may be penta- or hexacoordinate with (N,O) and (S,Cl) ligands and a heavier scatterer with the backscattering

characteristics of Se at a Ni–Se distance of 2.44 Å. A hexacoordinate, pseudo-octahedral Ni site is considered more probable, however, based on the best curve-fitting results of Table 1 and the assignment of the *D. baculatus* hydrogenase Ni EPR signals to a Ni site of distorted octahedral symmetry (19).

Analysis of the Se EXAFS confirms the presence of a first-row transition metal scatterer at a Se–M distance of $\approx 2.4 \text{ \AA}$ and also identifies a single C scatterer at a typical Se–C distance of 2.0 Å. The short range of Se EXAFS data limits our ability to accurately determine Se distances to heavy scatterers (the amplitude functions of which peak at high *k* values) and is probably the source of the discrepancy in the Ni–Se (2.44 Å) and Se–Ni (2.39 Å) distances. We interpret the Se EXAFS as a Se–Ni bond rather than a Se–Fe bond on the strength of the Ni EXAFS evidence for a Ni–Se bond. Further support for the existence of a Ni–Se bond has been confirmed in EPR experiments on [NiFeSe]hydrogenase isolated from *D. baculatus* grown on a medium supplemented with $^{77}\text{SeO}_3^{2-}$ (S. H. He, M. Teixeira, J.L., D. S. Patil, D.V.D., B. H. Huynh, and H.D.P., Jr., unpublished data). Thus, the best estimate of the [NiFeSe]hydrogenase Ni site composition is 3–4 (N,O) at 2.06 Å, 1–2 (S,Cl) at 2.17 Å, and 1 Se at 2.44 Å.

The presence of a single C scatterer in the Se environment strongly suggests that it is a selenocysteine residue coordinated to the [NiFeSe]hydrogenase Ni site. A recent reanalysis of the DNA sequence for the *D. baculatus* [NiFeSe]hydrogenase gene (J.L., H.D.P., Jr., G. Voordouw, N. K. Menon, E. S. Choi, and A. E. Przybyla, unpublished data) has identified a TGA codon, which has been shown to encode selenocysteine (43–45). The deduced protein sequence in the region of this codon is homologous to the same region of the [NiFe]hydrogenases (5), except that one of the positions normally occupied by a cysteine is occupied by the selenocysteine in the [NiFeSe]hydrogenase. Thus, two independent pieces of evidence support the existence of a Ni–selenocysteine bond in this hydrogenase. The presence of selenocysteine has been demonstrated in the hydrogenase of *Methanococcus vannielii* (46).

One of the major functional differences observed between the [NiFeSe]- and the [NiFe]hydrogenases is the $\text{H}_2/\text{H}^2\text{H}$ ratio measured in the $^2\text{H}_2\text{-H}^+$ exchange reaction (19, 20). This ratio is usually ≤ 0.5 for the [NiFe]hydrogenases but is significantly > 1 for the [NiFeSe]hydrogenases (19). Thus, the presence of selenocysteine has a significant effect on the catalytic activity, possibly through its close proximity to the “active site.” Our demonstration that the selenocysteine is directly coordinated to the Ni site in the [NiFeSe]hydrogenase strongly suggests that Ni is part of the active site of a Ni-containing hydrogenase.

The precise chemical explanation for the higher $\text{H}_2/\text{H}^2\text{H}$ ratio in the hydrogenases that contain Se will have to await further experimentation. A higher $\text{H}_2/\text{H}^2\text{H}$ ratio implies an increased labilization of the proposed nickel hydride intermediate (19), suggesting an effect of cysteine replacement by selenocysteine on the nickel electronic structure and, thus, the nickel hydride bond. Our Ni x-ray absorption edge

Table 2. Curve-fitting results for Se EXAFS of *D. baculatus* hydrogenase

Fit	Se–Ni			Se–Fe			Se–C			<i>f'</i>
	N_s	$R_{as}, \text{ \AA}$	$\Delta\sigma_{as}^2, \text{ \AA}^2$	N_s	$R_{as}, \text{ \AA}$	$\Delta\sigma_{as}^2, \text{ \AA}^2$	N_s	$R_{as}, \text{ \AA}$	$\Delta\sigma_{as}^2, \text{ \AA}^2$	
2A	—	—	—	(1)	2.34	0.0038	(1)	1.99	0.0000	0.062
2B	(1)	2.39	0.0080	—	—	—	(1)	1.97	0.0000	0.080

N_s is the number of scatterers per selenium; R_{as} is the selenium-scatterer distance; σ_{as} is a root-mean-square deviation in R_{as} ; $\Delta\sigma_{as}^2$ is $\sigma_{fit}^2 - \sigma_{model}^2$, where the models for Se–C, Se–Fe, and Se–Ni were PhSeSePh at ambient temperature, $\text{Fe}_2\text{Se}_2(\text{CO})_6$ at ambient temperature, and $[\text{Ni}(\text{Se}_2\text{C}_2(\text{CF}_3)_2)_2]^-$ at 10 K, respectively. The *k* range of the fits was $4-10 \text{ \AA}^{-1}$. *f'* is described in Table 1. Numbers in parentheses were not varied during optimization.

spectra of [NiFe]hydrogenase (22) suggest a very covalent environment, with a significant chalcogenide (S, Se) participation in the active site valence molecular orbitals. Redox changes at the active site must then involve the S, Se ligand atoms in addition to the Ni, providing the mechanism for the Se substitution influence on the catalytic activity.

The XAS work was done at the Stanford Synchrotron Radiation Laboratory, which is supported by the Department of Energy, Office of Basic Energy Sciences; and the National Institutes of Health, Biotechnology Resource Program, Division of Research Resources. XAS studies under R.A.S. were supported by National Science Foundation Grant DMB-8645819. R.A.S. is a National Science Foundation Presidential Young Investigator. The research was also supported by Contract DEA5-09-79-ER10499 from the Department of Energy to H.D.P., Jr., and a grant from the National Science Foundation (DMB-8706205) to H.D.P., Jr., J.L., and D.V.D.

- Adams, M. W. W., Mortenson, L. E. & Chen, J.-S. (1981) *Biochim. Biophys. Acta* **594**, 105–176.
- Odom, J. M. & Peck, H. D., Jr. (1981) *FEMS Microbiol. Lett.* **12**, 47–50.
- Prickril, B. C., He, S.-H., Li, C., Menon, N., Choi, E.-S., Przybyla, A. E., DerVartanian, D. V., Peck, H. D., Jr., Fauque, G., LeGall, J., Teixeira, M., Moura, I., Moura, J. J. G., Patil, D. & Huynh, B. H. (1987) *Biochem. Biophys. Res. Commun.* **149**, 369–377.
- Voordouw, G. & Brenner, S. (1985) *Eur. J. Biochem.* **148**, 515–520.
- Li, C., Peck, H. D., Jr., LeGall, J. & Przybyla, A. E. (1987) *DNA* **6**, 539–551.
- Menon, N. K., Peck, H. D., Jr., LeGall, J. & Przybyla, A. E. (1987) *J. Bacteriol.* **169**, 5401–5407.
- Huynh, B. H., Czechowski, M. H., Krüger, H. J., DerVartanian, D. V., Peck, H. D., Jr. & LeGall, J. (1984) *Proc. Natl. Acad. Sci. USA* **81**, 3728–3732.
- Van der Westen, H. M., Mayhew, S. G. & Veeger, C. (1978) *FEBS Lett.* **86**, 122–126.
- Glick, B. R., Martin, W. G. & Martin, S. M. (1980) *Can. J. Microbiol.* **26**, 1214–1223.
- LeGall, J., Ljungdahl, P. O., Moura, I., Peck, H. D., Jr., Xavier, A. V., Moura, J. J. G., Teixeira, M., Huynh, B. H. & DerVartanian, D. V. (1982) *Biochem. Biophys. Res. Commun.* **106**, 610–616.
- Teixeira, M., Moura, I., Xavier, A. V., DerVartanian, D. V., LeGall, J., Peck, H. D., Jr., Huynh, B. H. & Moura, J. J. G. (1983) *Eur. J. Biochem.* **130**, 481–484.
- Teixeira, M., Moura, I., Xavier, A. V., Huynh, B. H., DerVartanian, D. V., Peck, H. D., Jr., LeGall, J. & Moura, J. J. G. (1985) *J. Biol. Chem.* **260**, 8942–8956.
- Moura, J. J. G., Teixeira, M., Moura, I., Xavier, A. V. & LeGall, J. (1986) in *Frontiers in Bioinorganic Chemistry*, ed. Xavier, A. V. (VCH, Weinheim, F.R.G.), pp. 3–11.
- Krüger, H. J., Huynh, B. H., Ljungdahl, P. O., Xavier, A. V., DerVartanian, D. V., Moura, I., Peck, H. D., Jr., Teixeira, M., Moura, J. J. G. & LeGall, J. (1982) *J. Biol. Chem.* **257**, 14620–14622.
- Czechowski, M. H., Huynh, B. H., Nacro, M., DerVartanian, D. V., Peck, H. D., Jr., & LeGall, J. (1984) *Biochem. Biophys. Res. Commun.* **125**, 1025–1032.
- Reider, R., Cammack, R. & Hall, D. O. (1984) *Eur. J. Biochem.* **145**, 637–643.
- Teixeira, M., Moura, I., Fauque, G., Czechowski, M. H., Berlier, Y., Lespinat, P. A., LeGall, J., Xavier, A. V. & Moura, J. J. G. (1986) *Biochimie (Paris)* **68**, 75–84.
- Lissolo, T., Choi, E. S., LeGall, J. & Peck, H. D., Jr. (1986) *Biochem. Biophys. Res. Commun.* **139**, 701–708.
- Teixeira, M., Fauque, G., Moura, I., Lespinat, P. A., Berlier, Y., Prickril, B., Peck, H. D., Jr., Xavier, A. V., LeGall, J. & Moura, J. J. G. (1987) *Eur. J. Biochem.* **167**, 47–58.
- Berlier, Y., Fauque, G. D., LeGall, J., Choi, E. S., Peck, H. D., Jr. & Lespinat, P. A. (1987) *Biochem. Biophys. Res. Commun.* **146**, 147–153.
- Fisher, D. S. & Price, D. C. (1964) *Clin. Chem.* **10**, 21–31.
- Scott, R. A., Wallin, S. A., Czechowski, M., DerVartanian, D. V., LeGall, J., Peck, H. D., Jr., & Moura, I. (1984) *J. Am. Chem. Soc.* **106**, 6864–6865.
- Swenson, D., Baenziger, N. C. & Coucouvanis, D. (1978) *J. Am. Chem. Soc.* **100**, 1932–1934.
- Davis, W. M., Roberts, M. M., Zask, A., Nakanishi, K., Nozoe, T. & Lippard, S. J. (1985) *J. Am. Chem. Soc.* **107**, 3864–3870.
- Ram, M. S., Espenson, J. H. & Bakac, A. (1986) *Inorg. Chem.* **25**, 4115–4118.
- Barefield, E. K. & Wagner, F. (1973) *Inorg. Chem.* **12**, 2435–2439.
- McAuley, A., Norman, P. R. & Olubuyide, O. (1984) *Inorg. Chem.* **23**, 1938–1943.
- Zompa, L. J. & Margulis, T. N. (1978) *Inorg. Chim. Acta* **28**, L157–L159.
- Setzer, W. N., Ogle, C. A., Wilson, G. S. & Glass, R. S. (1983) *Inorg. Chem.* **22**, 266–271.
- Seyferth, D. & Henderson, R. S. (1981) *J. Organomet. Chem.* **204**, 333–343.
- Campana, C. F., Lo, F. Y.-K. & Dahl, L. (1979) *Inorg. Chem.* **18**, 3060–3064.
- Stern, E. & Heald, S. (1979) *Rev. Sci. Instr.* **50**, 1579–1582.
- Stern, E. A. & Kim, K. (1981) *Phys. Rev.* **B23**, 3781–3787.
- Scott, R. A. (1985) *Methods Enzymol.* **117**, 414–459.
- Teo, B.-K. & Lee, P. A. (1979) *J. Am. Chem. Soc.* **101**, 2815–2832.
- Knapp, S., Keenan, T. P., Zhang, X., Fikar, R., Potenza, J. A. & Schugar, H. J. (1987) *J. Am. Chem. Soc.* **109**, 1882–1883.
- Davison, A. & Holm, R. H. (1967) *Inorg. Synth.* **10**, 8–26.
- Hove, M. J., Hoffman, B. M. & Ibers, J. A. (1972) *J. Chem. Phys.* **56**, 3490–3502.
- Bonamico, M. & Dessy, G. (1971) *J. Chem. Soc. A*, 264–269.
- Marsh, R. E. (1952) *Acta Crystallogr.* **5**, 458–462.
- Eidsness, M. K., Sullivan, R. J. & Scott, R. A. (1988) in *Bioinorganic Chemistry of Nickel*, ed. Lancaster, J. R. (VCH, Deerfield Beach, FL), pp. 73–91.
- Smith, T. A., Penner-Hahn, J. E., Berding, M. A., Doniach, S. & Hodgson, K. O. (1985) *J. Am. Chem. Soc.* **107**, 5945–5955.
- Leinfelder, W., Zehelein, E., Mandrand-Berthelot, M.-A. & Böck, A. (1988) *Nature (London)* **331**, 723–725.
- Mullenbach, G. T., Tabrizi, A., Irvine, B. D., Bell, G. I. & Hallewell, R. A. (1987) *Nucleic Acids Res.* **15**, 5484.
- Chambers, I., Frampton, J., Goldfarb, P., Affara, N., McBain, W. & Harrison, P. R. (1986) *EMBO J.* **5**, 1221–1227.
- Yamazaki, S. (1982) *J. Biol. Chem.* **257**, 7926–7929.